Calcium current during a single action potential in a large presynaptic terminal of the rat brainstem

J. G. G. Borst and B. Sakmann

Max-Planck-Institut für medizinische Forschung, Abteilung Zellphysiologie, Jahnstrasse 29, D-69120 Heidelberg, Germany

(Received 30 June 1997; accepted after revision 15 September 1997)

1. The calcium current of a 'giant' synaptic terminal (the calyx of Held) was studied using two-electrode voltage clamp in slices of the rat brainstem.

2. In terminals with a long axon (length > 100 μm), the passive current transient decayed bi-exponentially following voltage steps. In terminals with a short axon (length < 30 μm), the slow component was reduced or absent. These terminals also had small slow calcium tail currents following long depolarizing voltage steps, suggesting that these are largely due to axonal calcium channels.

3. Terminals were voltage clamped with action potential waveform commands. At both 24 and 36 °C the calcium current began shortly after the peak of the action potential and ended before the terminal was fully repolarized.

4. The calcium current during the repolarization phase was 69 ± 1 % ($n = 3$) of maximal, judged from the increase in this current when a plateau phase was added to the action potential waveform.

5. A Hodgkin–Huxley m^2 model, based on the measured activation and deactivation of the calcium current, reproduced both the time course and the amplitude increase of the calcium currents during the different action potential waveforms well.

6. The fast gating of the calcium channels in the terminal ensures that they are effectively opened during the repolarization phase of an action potential. This implies that the distance between open calcium channels is minimized, which is in agreement with the view that multiple calcium channels are needed to release a vesicle in this synapse.

The main function of action potentials in synaptic terminals of the central nervous system (CNS) is to open voltage-dependent calcium channels in the vicinity of vesicles filled with neurotransmitter. The subsequent inflow of calcium triggers the release of these vesicles (Katz, 1969). This release depends very steeply on the calcium influx (Dodge & Rahamimoff, 1967). Therefore, the shape of the action potential and the gating properties of the calcium channels determine, to a large extent, how many vesicles will be released. In the squid giant synapse and in the calyx-type synapse of the chick ciliary ganglion presynaptic action potentials may open calcium channels rather ineffectively (Pumplin, Reese & Llinás, 1981; Bertram, Sherman & Stanley, 1996). For example, in the squid it was estimated that only 10 % of the available calcium channels are opened during an action potential (Pumplin *et al.* 1981). In contrast, it has been suggested that presynaptic calcium channels in the cerebellum activate so fast at physiological temperatures that they already begin to open early during the upstroke of the action potential and the peak of the calcium current almost coincides with the peak of the action potential (Sabatini & Regehr, 1996). As a result, open probability of these calcium channels would reach values that are close to maximal (Sabatini & Regehr, 1997).

In these two extreme cases, the regulation of synaptic strength by calcium influx is expected to be very different. If action potentials open calcium channels ineffectively, in between open calcium channels there will be many closed channels (Augustine, 1990). If the distance between open channels is relatively large, the high concentrations of calcium that are necessary for fast transmitter release are only attained adjacent to an open channel. This would mean that most vesicles are released due to the opening of a single calcium channel. On the other hand, if action potentials open calcium channels effectively, open calcium channels will be relatively close to each other and calcium that enters through adjacent channels may sum to enlarge the region in which the calcium concentration is sufficiently high to drive secretion (reviewed in Zucker, 1996).

Here we voltage clamp the calcium current in 'giant' presynaptic terminals (the calyces of Held) in rat brainstem

slices. These glutamatergic terminals are located in the medial nucleus of the trapezoid body (MNTB), which is part of a fast relay pathway (Forsythe & Barnes-Davies, 1993; Borst, Helmchen & Sakmann, 1995) that is involved in the localization of sound (Helfert & Aschoff, 1997). By pharmacologically isolating the calcium currents, it is possible to measure the calcium current that flows during a presynaptic action potential when an action potential is used as the voltage command (Llinás, Sugimori & Simon, 1982). Using this approach, we recently reported that at room temperature a large calcium current flows into the presynaptic terminal during the repolarization phase (Borst & Sakmann, 1996). Here we compare this with the current during an action potential at a more physiological temperature. Moreover, we relate the gating properties of the calcium channels, measured during step voltage changes, to the measured calcium current during an action potential. We were particularly interested in the question of what percentage of the calcium channels open during an action potential. We attempted to measure this using different command waveforms and by modelling the calcium current with a Hodgkin–Huxley kinetic scheme.

METHODS

Preparation of slices and two-electrode voltage clamp recordings from single presynaptic terminals (calyces of Held) were as described in Borst & Sakmann (1996), the only change being that slices were cut at an angle of around 20 deg with the coronal plane. The presence of an axon may severely compromise voltage clamp studies (Augustine, Charlton & Smith, 1985), especially since the axon that forms the calyx of Held has calcium channels, although they are most likely to be at a lower density than in the terminal (Borst *et al.* 1995). Since the afferent axons run in the coronal plane (Kuwabara, DiCaprio & Zook, 1991), their length will be reduced by cutting the slices at an angle with the coronal plane. In some cases we recorded from terminals without an axon. In contrast to our earlier studies (Borst *et al.* 1995; Borst & Sakmann, 1996), we did not pre-select terminals that were able to induce an action potential in the postsynaptic cell.

In brief the methods used to prepare slices and to voltage clamp terminals were as follows.

Eight- to ten-day-old Wistar rats were decapitated without prior anaesthesia using a small animal guillotine. Slices were cut from their brainstem and transferred to a recording chamber, and during recordings of the calcium current, they were perfused with a solution containing (mM): 105 NaCl, 20 TEACl, 0·1 3,4-diaminopyridine, 2·5 KCl, 1 $MgCl_2$, 2 $CaCl_2$, 25 dextrose, 1·25 NaH_2PO_4, 0·4 ascorbic acid, 3 *myo*-inositol, 2 sodium pyruvate, 0·001 tetrodotoxin (TTX), 25 $NaHCO_3$, pH 7·4 when bubbled with 95% O_2, 5% CO_2. Bath temperature was 23–24 °C unless noted otherwise. In three experiments, bath temperature was raised to 36 ± 1 °C by pre-warming the saline before it entered the recording chamber. In these experiments, temperature was monitored with a thermistor placed in the vicinity of the slice.

Presynaptic two-electrode voltage clamp recordings were made with an Axoclamp-2B amplifier, using two HS-2A x0·1L headstages. Whole-cell recordings were established with two different patch pipettes in the same terminal; one electrode was used for injecting current and the other one for monitoring voltage. Pipettes (9–12 MΩ, coated with Sylgard) were at least 8 μm apart. Capacitive coupling between the electrodes was minimal up to a bandwidth of 5 kHz, as judged by injecting sine waves of different frequencies into one of the electrodes and monitoring the size of the response in the other one (Neher, 1970). Electrodes were filled with a solution containing (mM): 115 caesium gluconate, 20 CsCl, 10 Na_2-phosphocreatine, 4 MgATP, 0·3 GTP, 0·05 BAPTA, 10 Hepes (pH 7·2 with CsOH) and 0·3 mg ml^{-1} Lucifer Yellow (Sigma, potassium salt). In some experiments 10 mM BAPTA was used, with no obvious differences on the currents that flow during a single action potential. In this case the caesium gluconate concentration was reduced to 90 mM to maintain osmolality at around 290 mosmol kg^{-1}. Caesium gluconate was purified by at least three precipitations in methanol. At the end of each experiment, axon length was estimated using the micrometer in the eyepiece of the microscope during epi-fluorescence illumination. In some experiments no axon could be seen. The absence of an axon was then confirmed by making a stack of images with a cooled CCD camera.

As the waveform command we used the presynaptic action potential displayed in Fig. 2*A* of Borst *et al.* (1995), interpolated to 20 μs per point with a cubic spline function. At 36 °C we used the one displayed in Fig. 3 of the same paper. In both cases the membrane potential during these earlier current clamp experiments was close to −80 mV, the holding potential in the present voltage clamp experiments. Potentials were corrected for a junction potential of −11 mV. Both of the two action potentials are representative of action potentials measured in the series of experiments described in Borst *et al.* (1995), as shown by a comparison of their properties. At 23–24 °C the maximal rate of rise of the action potential was 654 V s^{-1}, and in a total of ten experiments from the same series, it was 584 ± 21 V s^{-1}. Half-width was 0·49 and $0·54 \pm 0·02$ ms and amplitude was 116 and 117 ± 2 mV for the action potential that was used as a template and for the total population, respectively. At 36 °C, maximum rate of rise was 1274 V s^{-1} for the action potential that was used as a template and 1018 ± 64 V s^{-1} for the total of five experiments; half-width was 0·25 and $0·26 \pm 0·02$ ms and peak amplitude was 112 and 110 ± 1 mV for the template action potential for the total, respectively.

No series resistance compensation was used. To speed up the voltage clamp and to allow the use of a higher gain to reduce series resistance errors, the voltage transients were allowed to overshoot (Fröhr, 1985); maximum overshoot was 10%. Errors due to series resistance were less than 10 mV. For a 10 mV step, 20–80% rise time was < 100 μs.

Subtraction of the passive response was by the *P*/5 method (Llinás *et al.* 1982). In addition, five inverted action potentials with a size one-fifth of the full action potential were also given (Fig. 5*A*) as a check on the symmetry of the passive response. In agreement with our earlier data (Borst & Sakmann, 1996), the *P*/5 current differed by < 1% from the *P*/−5 current and matched the first derivative of the voltage transient well, and therefore it is most likely to represent the current needed to charge the presynaptic membrane (plus a small leak current). The small difference in the passive component of the currents during action potential waveforms that resulted from the slower repolarization in the presence of calcium currents could be neglected. The difference between the *P*/5 current and the full waveform current was almost completely blocked by Cd^{2+} (0·2 mM, $n = 7$); the residual current may be due to the less potent block of the calcium current by Cd^{2+} at negative voltages (Brown, Tsuda & Wilson, 1983; Byerly, Chase & Stimers, 1984).

The inter-pulse interval was 10–15 s. The calcium current showed little rundown in most experiments, except when steps with a duration longer than 10 ms were used in the peak current–voltage (I–V) relation. I–V relations and action potential waveform currents were generally recorded between 5 and 10 min after break in.

Currents were filtered at 5 kHz, voltages at 10 kHz (8-pole Bessel filter). In some figures currents have been digitally filtered to 500 Hz or 1 kHz, as indicated. Currents were digitized at 20 μs per point with a 16-bit analog-to-digital converter (ITC-16, (Instrutech, Greatneck, NY, USA).

Analysis

Acquisition and analysis were done with Pulse Control 4.6 (Herrington & Bookman, 1994) and Igor (WaveMetrics, Lake Oswego, OR, USA) macros. For the analysis of action potential waveform voltage clamp experiments, the maximum rate of voltage rise and the maximum current were aligned to correct for the different filtering of the voltage and current recording. This involved a correction of less than 30 μs.

Peak of the current–voltage (I–V) relation was obtained by interpolation with a cubic spline function.

An estimate for the capacitance of the terminal 'seen' during the action potential waveform command was obtained by scaling the peak of the first derivative of the measured voltage to the peak of the outward current during the action potential waveform, using $C = I/(\mathrm{d}V/\mathrm{d}t)$, where C is capacitance, I is current (corrected for leak) and $\mathrm{d}V/\mathrm{d}t$ is the time derivative of the voltage. Using the integral of current and $\mathrm{d}V/\mathrm{d}t$ during the rising phase of the action potential waveform gave similar results ($< 5\%$ difference, $n = 19$).

Simulation of calcium currents

Simulation of currents during an action potential was done largely as described by Hodgkin & Huxley (1952). Calcium currents were modelled with a Hodgkin–Huxley (HH) model. The HH model provides a simple way to describe the overall properties of the calcium currents. This model neglects any heterogeneities within the calcium channel population (Wu, Borst & Sakmann, 1997). We chose a model with two gating particles, called m, and no inactivation, because it has been used successfully to describe the calcium current in other preparations (e.g. Byerly *et al.* 1984; Kay & Wong, 1987; Sala, 1991; Zidanic & Fuchs, 1995), and because the onset of activation at positive potentials was better described by a model with two gates than with one or three gates when the traces were filtered at 2 kHz. At 5 kHz, the differences between the models with one, two or three gates were not very obvious, partly due to the lower signal-to-noise ratio.

For the construction of the HH model, deactivation of the calcium current during steps from 0 mV to voltages between −20 and −60 mV was fitted using (Hodgkin & Huxley, 1952):

$$I(t) = [\sqrt{I_\infty} - (\sqrt{I_\infty} - \sqrt{I_0})\exp(-t/\tau_m)]^2, \quad (1)$$

where t is time, I_∞ is steady-state current, I_0 is current at $t = 0$ (in this case the peak of the tail current) and τ_m is the time constant describing the exponential relaxation of gate m after a voltage step. Fitting was started 80 μs after the peak of the tail current. At this point, inward 'asymmetry' currents had largely subsided.

Activation of the calcium current was measured during 10 ms steps from −80 mV to potentials between −30 and +30 mV. Since I_0 is close to zero at the holding potential of −80 mV, eqn (1) simplifies to:

$$I(t) = I_\infty[1 - \exp(-t/\tau_m)]^2. \quad (2)$$

After stepping back to −80 mV, fast inward tail currents were observed. They were integrated over 0·5 ms and normalized to the amplitude of the largest integral. The integrals were used as a measure for steady-state activation because the speed of the voltage clamp was not sufficient to measure accurately the peak of the tail currents (Augustine *et al.* 1985). At the beginning of the step, outward 'asymmetry' currents were generally seen. We assumed that these would also be present when stepping back to the holding potential, contributing to the tail currents. Therefore the integral of the outward current at the beginning of the step was subtracted from the tail current integral. No correction was made for inactivation of the calcium current during the 10 ms steps. The average steady-state activation parameter $\bar{m}^2_\infty$ was obtained from the averaged, normalized tail current integrals by fitting them with a squared Boltzmann function:

$$\bar{m}^2_\infty = 1/\{1 + \exp[(V_\mathrm{h} - V)/\kappa]\}^2, \quad (3)$$

where V is membrane potential, V_h is the half-activation voltage and κ is the steepness factor.

The rate constants of the HH model, α_m and β_m, were calculated from τ_m and $\bar{m}^2_\infty$ according to:

$$\alpha_m = \bar{m}^2_\infty/\tau_m, \quad (4)$$

$$\beta_m = (1 - \bar{m}_\infty)/\tau_m \quad (5)$$

where α_m is the rate at which gate m opens, and β_m the rate at which it closes. The dependences of α_m and β_m on voltage were fitted with exponential functions:

$$\alpha_m = \alpha_0\exp(V/V_\alpha), \quad (6)$$

$$\beta_m = \beta_0\exp(-V/V_\beta). \quad (7)$$

Since α_m increases and β_m decreases with voltage, the steady-state open probability ($\alpha_m/(\alpha_m + \beta_m)$) must approach 1 at very positive voltages. However, calcium channels always show bursts of openings in single-channel recordings, so the peak open probability is likely to be less than 1. Therefore, the open probabilities described here or in Pumplin *et al.* (1981) are relative to the maximum possible open probability, which may be as high as 0·7 under some conditions (e.g. Delcour, Lipscombe & Tsien, 1993).

The calculated α_m and β_m were used to obtain m during an action potential by numerical integration of (Hodgkin & Huxley, 1952):

$$\mathrm{d}m/\mathrm{d}t = \alpha_m(1 - m) - \beta_m m, \quad (8)$$

where m is a dimensionless variable, which can vary between 0 (closed) and 1 (open), m_0 was set to 0 and the integration time step was 20 μs.

From the open probability of calcium channels (m^2) during the action potential waveforms, the currents were calculated with:

$$I(t) = m^2 g_\mathrm{max}(V - V_\mathrm{r}). \quad (9)$$

The maximal conductance g_max and the reversal potential V_r were obtained by fitting the peak amplitudes (I_peak) in the averaged I–V in the range −80 to +30 mV, the range relevant for action potentials, with:

$$I_\mathrm{peak} = \bar{m}^2_\infty g_\mathrm{max}(V - V_\mathrm{r}). \quad (10)$$

Fitting was done with the Levenberg–Marquardt algorithm that is built into Igor. Points were weighed by the inverse of their variance, when possible.

RESULTS

Passive properties

Giant terminals were voltage clamped and their calcium currents were pharmacologically isolated. The fluorescent dye Lucifer Yellow was included in the pipette solution and at the end of each experiment the length of the axon was estimated using the micrometer in the microscope's eyepiece. On the basis of this estimate, the terminals were initially divided into three groups. In the first group the axon had been cut within 30 μm from the terminal. The terminal with the longest axon in this group is shown in Fig. 1*A*. In the second group the axon was longer, around 100–300 μm. In the third group the cut end of the axon could not be traced, but the axon length was at least 200 μm. The results obtained with the terminals in the second and third group were very similar, so they were pooled. In addition, they were very similar to those of the terminals that were described in Borst & Sakmann (1996), in which case the axon extended to the mid-line and the terminals were shown to be 'functional', i.e. upon afferent

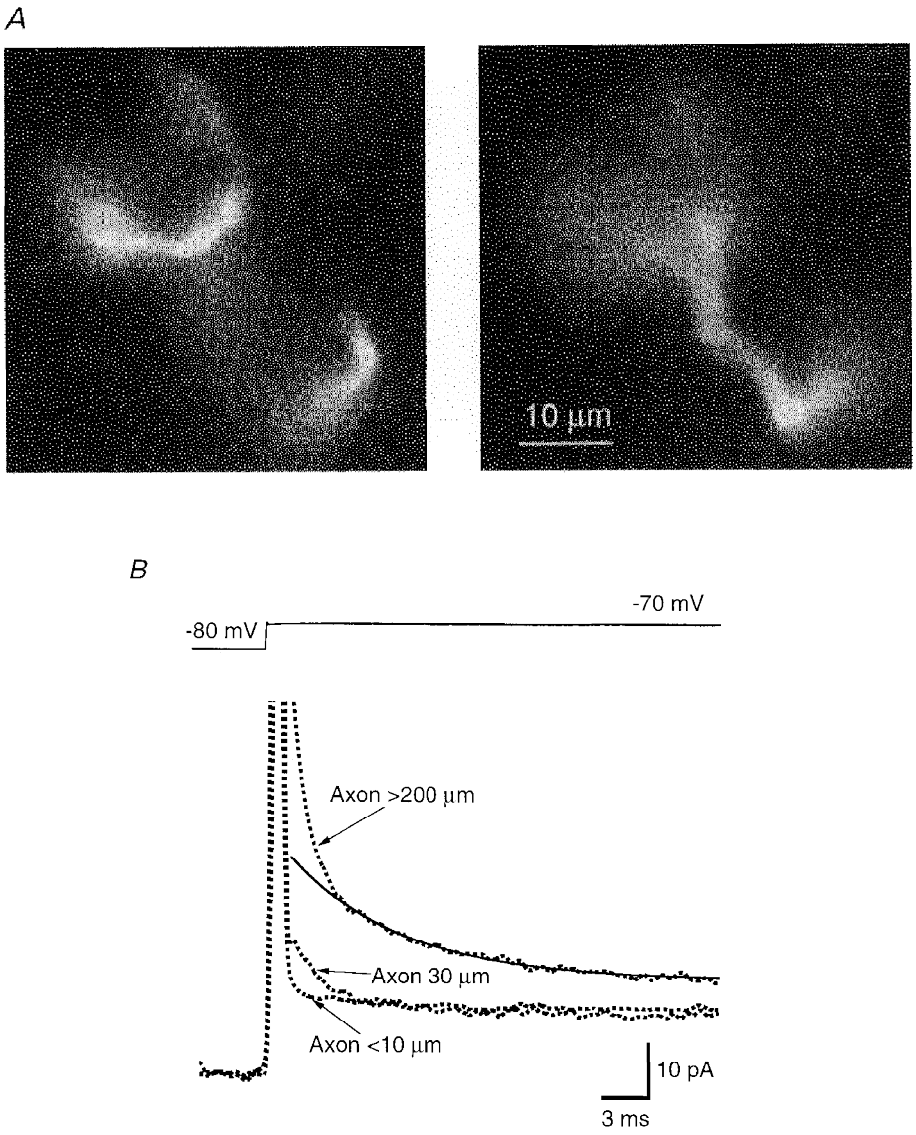

Figure 1. Terminals with and without an axon

A, fluorescent images of a terminal in which the axon length was around 30 μm. Left image shows the calyx (top left) and the tip of the axon, which had been cut at the surface of the slice (lower right). Right image shows the axon, beneath the surface of the slice. *B*, passive properties. Top, voltage measured with a separate electrode; average of 25 steps from −80 to −70 mV. Bottom, dotted lines, currents digitally filtered at 500 Hz for display. Continuous line is the fit with a single exponential function with a time constant of 7·4 ms. In the terminal that possessed an axon with a length of more than 200 μm, the charging of the membrane had a slow component, which was not present in the terminal in which the axon had been cut less than 10 μm from the terminal. A smaller slow component is present in the calyx shown in *A*.

stimulation they released enough vesicles to evoke an action potential in the postsynaptic cell.

Passive membrane properties of the terminals were measured with a 50 ms, 10 mV step from the holding potential of −80 mV. Input resistance was 1·2 ± 0·3 GΩ ($n = 7$; mean ± S.E.M.) in the absence and 1·0 ± 0·2 GΩ ($n = 17$) in the presence of an axon. Total capacitance, calculated from the current integral, was 23·8 ± 2·7 and 43·3 ± 2·9 pF, respectively. Not only was the total capacitance of terminals with an axon clearly larger, it also took much longer to charge them (Fig. 1*B*). The slow component in the charging transient could be described by an exponential function with a time constant of 5·6 ± 0·7 ms. This slow component made up around half of the total charge. In contrast, in terminals without an axon, this slow component was strongly reduced, or absent (Fig. 1*B*). Total capacitance was much smaller than in terminals with an axon and they were almost completely charged within 0·2 ms ($n = 7$). Therefore, the slow phase most likely represents the slow charging of the axonal membrane.

Calcium currents

Calcium currents were studied using a standard voltage step protocol. The membrane potential was stepped to various potentials for 10 or 150 ms (Fig. 2). Threshold for activation of the calcium currents was at around −40 mV, the peak was at around 0 mV and peak amplitude of inward currents was −1·9 ± 0·1 nA ($n = 18$), in agreement with earlier results (Borst *et al.* 1995; Borst & Sakmann, 1996; Helmchen, Borst & Sakmann, 1997). The currents reversed at around +60 mV, showing that there was little contribution of potassium currents to the measured currents. At positive potentials fast, short-lasting, outward 'asymmetry' currents appeared, which made a detailed analysis of the time course of activation more difficult. They may partly be due to a gating current. In addition, in some terminals there was a small residual transient inward component (not shown), which may be due to incomplete block of the sodium current by TTX. These terminals were not included in the analysis of activation.

Activation

At −30 mV, around the threshold for activation, the inward current activated rapidly, with time constants around

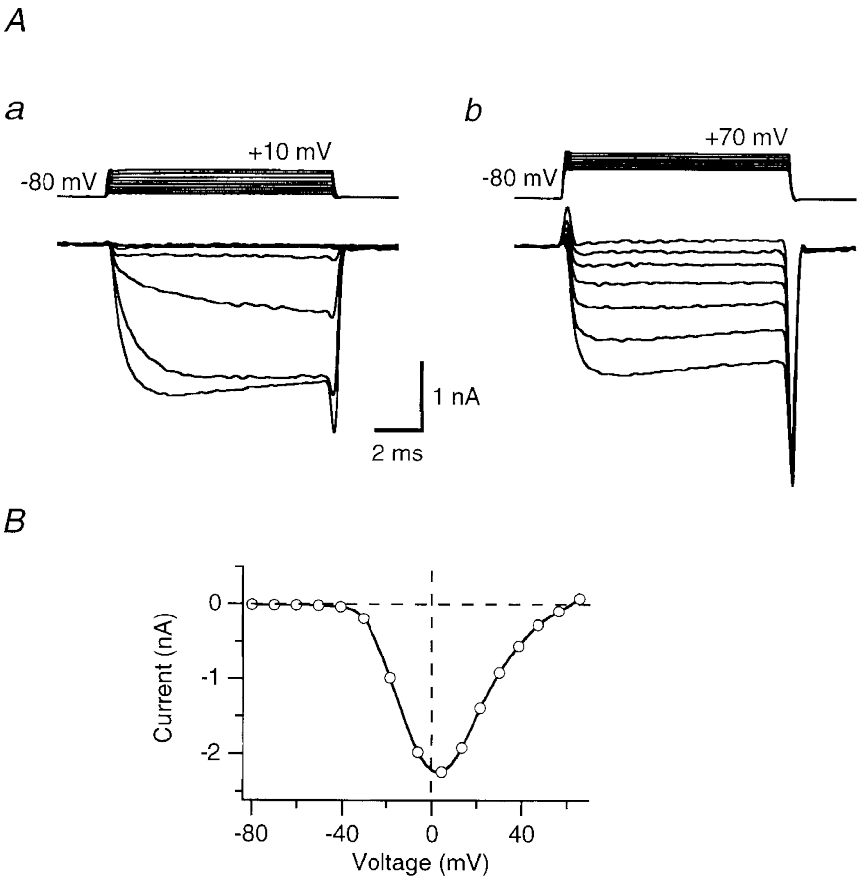

Figure 2. *I–V* of calcium channels in the absence of an axon

Leak and capacitative currents were subtracted on-line with a *P*/5 protocol. Filtered at 1 kHz for display. *A*, current traces (bottom) and voltage traces (top), recorded with two separate pipettes during 10 ms steps from a holding potential of −80 mV. *Aa*, steps from −70 to +10 mV. *Ab*, steps from +20 to +70 mV. *B*, *I–V* of peak amplitudes of the traces shown in *A*.

0·25 ms ($n = 7$). At this potential, the current showed only small or no inactivation for steps with a duration of 150 ms. The inward current at −30 mV can be identified as a calcium current on the basis of experiments in which calcium influx was detected with fluorescence methods (see Fig. 4 of Helmchen *et al.* 1997) and its block by 0·2 mM Cd^{2+}. At −20 mV the calcium current activated biphasically, with a faster time constant around 0·4 ms, and a slower time constant of around 2 ms (Fig. 3). At more positive potentials activation became faster again and at these potentials its time course of activation could be reasonably well fitted by a single exponential function (Fig. 3). At +30 mV, which is close to the most positive potential reached during action potentials (Borst *et al.* 1995), the time constant was 0·18 ± 0·02 ms.

Deactivation

Deactivation was studied by stepping the membrane potential to voltages in the range −60 to −20 mV after a 5 ms step to 0 mV. Three components could be distinguished in the tail currents. The fastest component is most likely to correspond to the deactivation of the calcium channels in the calyx. This component became faster with more negative potentials (Fig. 4). Terminals with an axon had a slow tail current with a time course similar to the slow component in the passive response (see also Fig. 6*B* of Borst *et al.* 1995). The amplitude 5 ms after stepping back to −80 mV amounted to around 6% of the peak amplitude ($n = 17$). In terminals that did not meet the criteria for sufficient voltage clamp (see Methods) this component was generally much larger and it outlasted the slow component in the charging transient. This component was not blocked by including 10 mM BAPTA in the pipette or by replacing Ca^{2+} by Ba^{2+} (not shown), suggesting that it did not result from a calcium-activated mechanism. Its absence in terminals without an axon (Fig. 2) suggests that this component resulted from poorly voltage clamped calcium channels in the axon. The third and slowest component in the tail currents was also present in terminals without an axon. It lasted tens of milliseconds. Peak amplitude was around 50 pA, reached following steps to 0 mV. It depended on intracellular calcium build-up, since it was reduced or absent when the pipette contained 10 mM BAPTA or when Ba^{2+} replaced Ca^{2+} as the charge carrier (not shown).

When fast deactivation was fitted with a single exponential function, time constants ranged from 0·61 ± 0·06 ms ($n = 4$) at −20 mV to 0·14 ± 0·02 ms at −50 mV. We obtained similar results with a protocol in which the repolarization phase of the action potential waveform command was ended at different negative potentials ($n = 4$, not shown). During voltage steps to potentials more

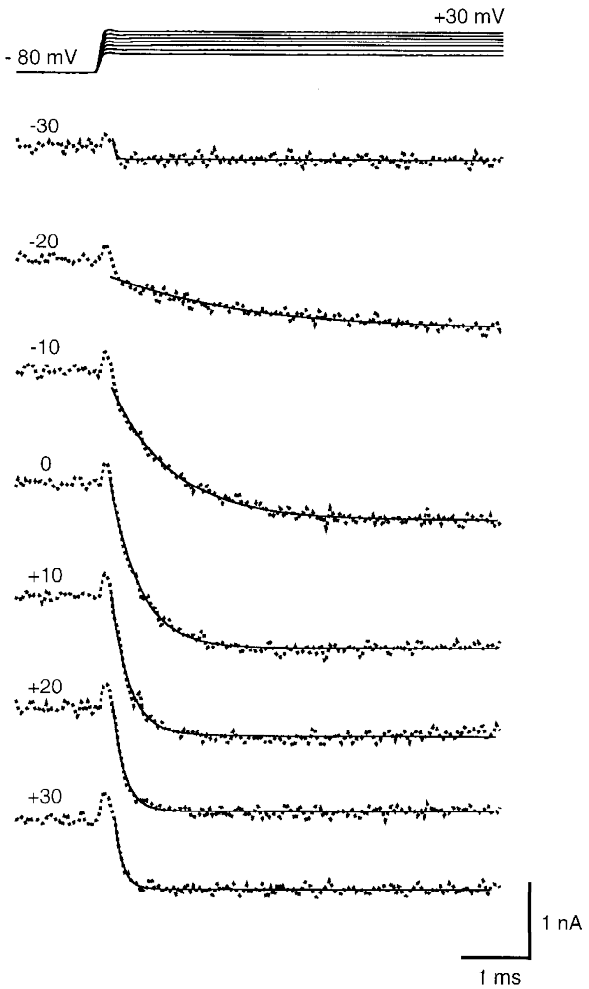

Figure 3. Activation of calcium currents

Same *I–V* curve as shown in Fig. 2, but filtered at 5 kHz. Top traces, recorded voltages. Holding potential −80 mV. Bottom traces: dotted traces, currents; continuous lines, fit of the onset of the calcium currents with a single exponential function. The fit was started where currents crossed the baseline, following the 'asymmetry' currents. Numbers to the right give the command voltage (in mV) during the step. Except for the step to −20 mV, fits are adequate. Time constants of the fits were (ms): 0·04 (−30 mV), 1·95 (−20 mV), 0·90 (−10 mV), 0·44 (0 mV), 0·27 (+10 mV), 0·18 (+20 mV), 0·12 (+30 mV).

negative than −50 mV, deactivation became too fast to be accurately resolved (time constant < 0·1 ms).

Action potential waveforms

To measure the influx of calcium during a presynaptic action potential, terminals were voltage clamped using action potential waveforms as command voltages. Figure 5*A* shows the standard waveform. The full action potential is preceded by five scaled and five scaled and inverted action potentials. The scaled action potentials were below the activation threshold of the calcium channels; they were used to measure the passive response of the terminals. Total currents are shown in Fig. 5*B* (middle panel). The calcium current can be isolated by subtracting the passive response from the total current needed to generate the full action potential (Fig. 5*B*, lower panel). The current began shortly after the peak of the action potential, peaked at a membrane potential of around −30 mV and ended before the terminal was fully repolarized, in agreement with earlier results (Borst & Sakmann, 1996). An outward 'asymmetry' current (on average 0·2 nA) preceded the calcium current. This may be partly due to a gating current (Toth & Miller, 1995; cf. Fig. 2*A*). Peak amplitudes of inward currents were −2·5 ± 0·1 nA ($n = 19$). The currents were on average 30 ± 4 % larger than the peak amplitudes of the *I–V* relations in the same experiment. The current integral was 0·92 ± 0·05 pC and the half-width was 0·36 ± 0·01 ms. The current could be well described by a Gaussian function with a standard deviation of 209 ± 4 μs. There were no significant differences (*t* test, $P > 0{\cdot}05$) in time course (half-width or standard deviation of the Gaussian), amplitude or current integral of the calcium current during an action potential between terminals with ($n = 14$) and without ($n = 5$) an axon, or with the terminals that had an axon that extended to the mid-line and had been shown to be able to induce a suprathreshold EPSP in the postsynaptic cell (Borst & Sakmann, 1996). This suggests that poorly clamped calcium channels in the axon do not contribute to the measured calcium current during action potential waveforms.

Two reasons could account for the similarity of the currents in the terminals with and without axons. Firstly, the calcium channel density in the axon is probably much lower than in the terminal (Borst *et al.* 1995). Secondly, the voltage clamp in the axon is probably so slow that during the action potential waveform the threshold for activation is not reached in most of the axon, since the time constant of the slow component in the passive transient is much slower than the half-width of the action potential (5·6 *vs.* 0·5 ms). A further indication that the action potential waveform is too fast to activate a substantial fraction of the axonal calcium channels comes from the fraction of the total capacitance that is 'seen' by the recording electrodes during the action potential waveforms. An estimate for this value can be obtained by scaling the (passive) currents to the first derivative of the voltage (see Methods). In terminals without an axon this value for the capacitance was on average 91 ± 2 % of the value obtained by integrating a step pulse, whereas in terminals that had an axon

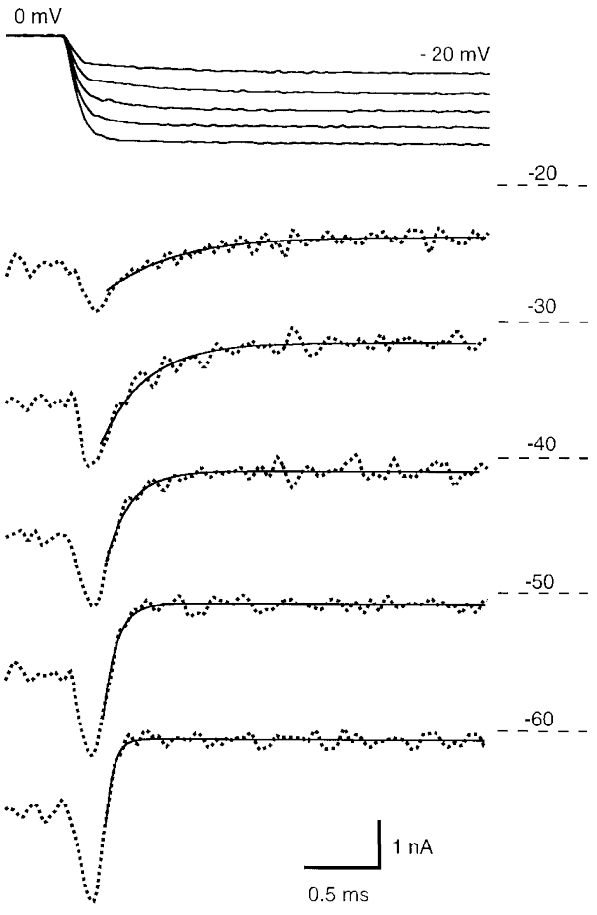

Figure 4. Deactivation of calcium currents

After a 5 ms step to 0 mV, the membrane potential was stepped back to potentials between −20 and −60 mV. Top, recorded voltage traces; bottom, currents. Continuous lines are the fit of a single exponential function. The beginning of the fit was 80 μs after the peak of the tail current. Time constants of the fits were (ms): 0·47 (−20 mV), 0·32 (−30 mV), 0·17 (−40 mV), 0·09 (−50 mV), 0·05 (−60 mV). Dotted lines indicate zero current levels for each trace.

attached, this value was only 68 ± 2%. Nevertheless, since total capacitance of terminals without an axon was only 55% of terminals with an axon, some of the capacitance that is 'seen' during an action potential waveform command in a terminal with an axon may come from the axon. At this developmental stage terminals still contain growth cones (Morest, 1968). These were not taken into consideration, but it may be that in terminals in which the axon is cut, more of the growth cones were cut as well. In that case we would overestimate the contribution of the axon to the total capacitance.

Calcium influx at physiological temperatures

All experiments described so far were done at the unphysiological temperature of 23–24 °C. To measure calcium influx under more physiological conditions, three terminals were voltage clamped at 36 °C. Peak amplitude of *I–V* relations was −2·9 ± 0·4 nA, reached at around −7 mV. To study calcium influx during action potentials, an action potential waveform was used that had previously been recorded (Borst *et al.* 1995) at the same temperature. The calcium current began shortly after the peak of the action potential and ended before repolarization was complete (Fig. 6). Its peak amplitude was −4·5 ± 0·2 nA, reached at around −30 mV. The current integral was 0·81 ± 0·02 pC. Its half-width was 0·17 ± 0·01 ms. The current could be well described by a Gaussian function with a standard deviation of 102 ± 5 μs.

How effectively do action potentials open calcium channels?

To test how much the calcium currents during the repolarization of the action potential can possibly increase, the duration of the peak of the action potential waveform command was prolonged (Fig. 7*A*). The rising phase and the repolarization phase were not changed. This experiment was also done with a plateau voltage to +60 mV. At room temperature, the normal action potential evoked a calcium current that was 69 ± 1% of maximal ($n = 3$). A plateau phase of less than 1 ms to +33 or +60 mV was sufficient to evoke a current that was close to maximal (Fig. 7*C*). Similar results were obtained for the current integrals.

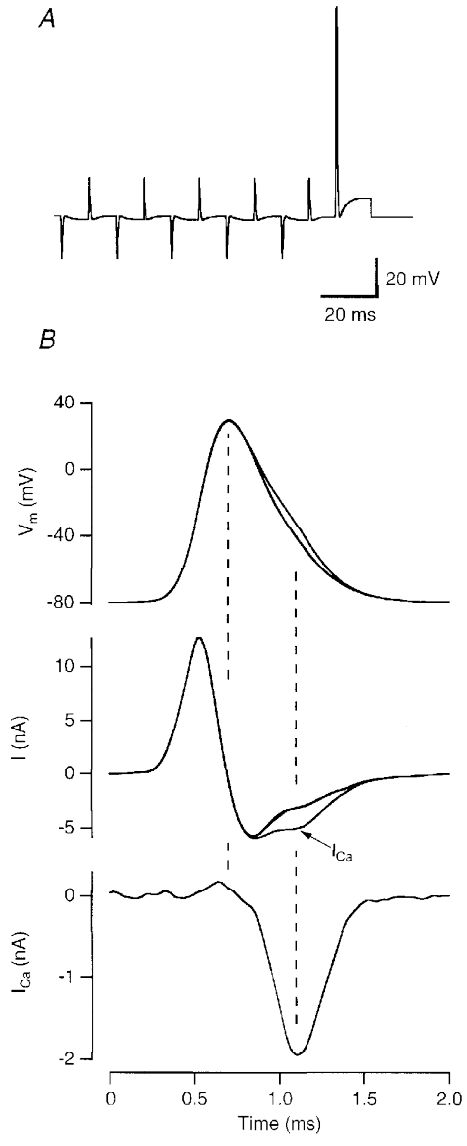

Figure 5. Calcium current during an action potential waveform command

Same terminal as shown in Fig. 1*A*. *A*, command template. The full-sized action potential is preceded by 5 reduced and 5 reduced and inverted action potentials, which were used for subtraction of the passive current. The −10 mV step at the end of the command was used to assess the speed of the voltage clamp. *B*, top, recorded voltages. Due to series resistance, the repolarization is somewhat slower during the full action potential than during the smaller (summed) action potentials. Middle, currents. The current flowing during the full-sized action potential has a larger inward component (labelled I_{Ca}). The two passive transients overlay well. Bottom, calcium current. The calcium current was obtained by subtracting the passive current from the current measured during the full action potential. A small outward current precedes the calcium current. All traces are the average of 11. Vertical dotted lines denote peak of the action potential waveform and of the calcium current.

Simulations

To relate the gating properties of the calcium channels to the current observed during an action potential, we modelled the currents with a Hodgkin–Huxley (HH) scheme, as described in Methods. A measure for the steady-state activation parameter was obtained from the integral of the tail currents and it was fitted with a squared Boltzmann function (Fig. 8*A*). We used the time constants (τ_m) of the fits of the activation and the deactivation of the calcium current in combination with the average steady-state activation parameter to obtain values for the rate constants of the HH scheme. At −30 and −20 mV the estimates for the time constants for activation and deactivation did not match very well (see above), contrary to the prediction of the HH model. At −30 mV the time constant (τ_m) for activation was faster than for deactivation. At −20 mV the fast component of the activation was faster, but the slow component was clearly slower than the deactivation. At these negative voltages we used the deactivation time constants (τ_m) to calculate α_m and β_m, since we assume that they better reflected the average behaviour of the total population of calcium channels. A step from −80 to 0 mV, as used in the deactivation protocol, will open almost all activatable channels, whereas a depolarizing step to, for example, −30 mV, as used for quantifying the activation, is likely to activate only a subpopulation of the channels.

The rate constants could be well fitted with exponential functions (Fig. 8*B*). In Fig. 8*C*, the observed and predicted time constants (τ_m) are compared, showing that the model matched the experimental results reasonably well.

To calculate current amplitudes from channel open probabilities, the maximal calcium conductance and the apparent reversal potential were obtained from the averaged *I–V* (Fig. 8*D*).

The exponential functions that described the dependency of the rate constants α_m and β_m on voltage were used to calculate the open probability (m^2) during an action potential by numerical integration of eqn (8) (Fig. 9). The time course of the simulated and the measured calcium current matched well (Fig. 9, lower traces). Half-width of the simulated current was 0·37 ms. It was well fitted with a Gaussian function with a standard deviation of 212 μs. The peak amplitude was reached at a membrane potential of −30 mV. However, in the simulations, channels closed somewhat faster than the measured ones. The predicted τ_m at −80 mV is only 34 μs (17 μs for a single exponential function. This value depends on the type of function used to extrapolate from the time constants obtained at −50 mV and more positive voltages (Fig. 8*B*), so it may not be accurate. Alternatively, the measured currents may have been slower than the simulated currents due to clamp speed being limiting during the last phase of the current.

Peak amplitude of the simulated current during the standard action potential waveform was −2·2 nA (Fig. 9, lower thin trace). This is only 19% larger than the peak amplitude in the simulated *I–V* relations (not shown), whereas the peak amplitude of the measured current was 30 ± 4% larger than the peak amplitude of the measured current–voltage relations. A possible explanation for the difference could be that the measured current is contaminated by a small inward 'asymmetry' component similar to the outward current that preceded the calcium current.

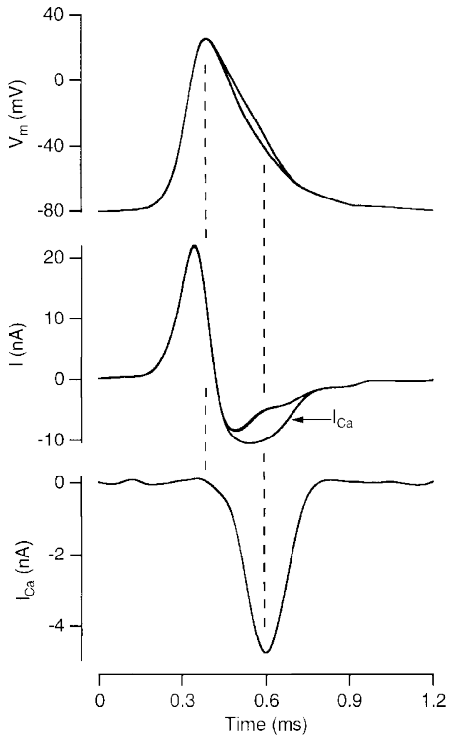

Figure 6. Calcium current during an action potential at 36 °C
Top, recorded voltages. Middle, currents. Bottom, calcium current. See legend of Fig. 5*B* for further details.

Peak open probability (m^2) of the channels was 0·69 (Fig. 9, middle traces, thin line). It was reached 0·24 ms after the peak of the action potential, at a membrane potential of around −10 mV. The increase of the amplitude of the simulated and the measured calcium current when action potentials contained a plateau agreed well, as illustrated in Fig. 9 (lower traces).

DISCUSSION

Voltage clamp of large terminals

We have previously shown that the presynaptic calcium current in the calyx of Held is of the high voltage-activated type and that it shows fast activation and deactivation (Borst *et al.* 1995). We confirm this under improved spatial and temporal voltage clamp conditions. We find that a slow component in both the passive transient and the calcium tail currents is largely due to slow charging of the axonal membrane. Alternative explanations, that this component is an inherent property of the calcium currents or that it is due to a calcium-activated current, are less likely since it was strongly reduced or absent in terminals without an axon and seemed not to be affected by the presence of 10 mM BAPTA intracellularly. In addition, there was a small component to the tail current which was also present in terminals without an axon and which was dependent on intracellular calcium build-up. The fast deactivation of calcium currents in terminals without an axon suggests that the growth cones which are still seen at this developmental stage (Morest, 1968) do not carry a significant fraction of the calcium current that was measured at the calyx.

In principle it is possible to voltage clamp the terminals, but we find even at room temperature that upon stepping back to potentials more negative than −50 mV, the currents deactivate almost completely within 100 μs, and are therefore too fast to be resolved accurately under the present recording conditions. Fortunately, the quality of the voltage clamp using action potential waveforms does not have to be as high as in the case of (long-lasting) voltage

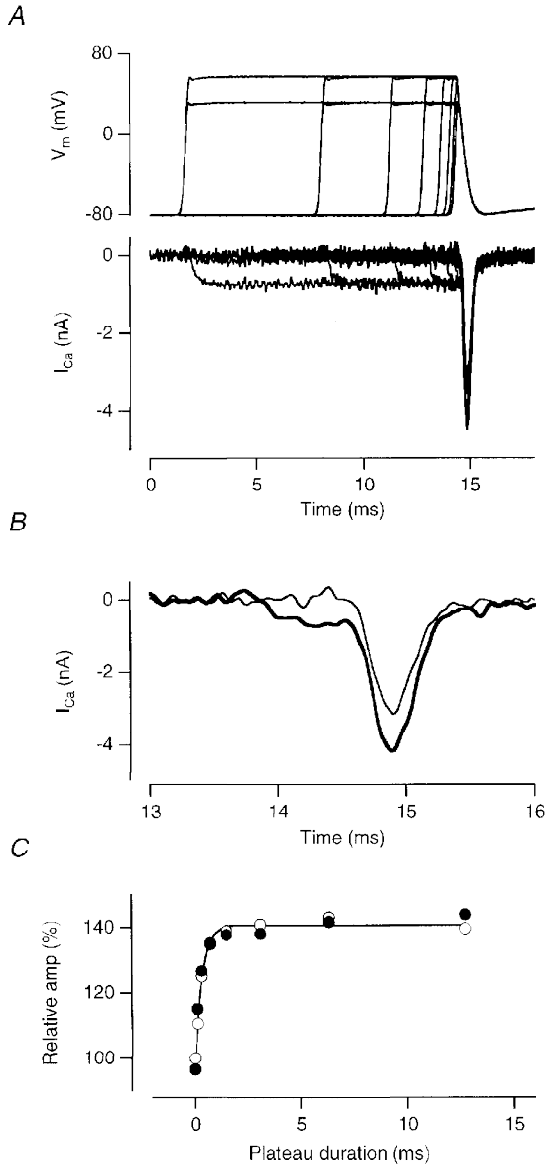

Figure 7. Action potentials open calcium channels effectively

The plateau phase of the action potential waveform was prolonged to find the maximal possible increase in the current during the repolarization phase. To ensure full activation of the calcium currents, action potential waveforms with a plateau phase of +60 mV were also tested. *A*, top, recorded voltages. Bottom, currents. During the plateau phase at +60 mV inward currents were very small, since this potential is close to the reversal potential of the calcium currents. *B*, calcium currents during the repolarization phase for the normal action potential waveform (thin trace) and for an action potential waveform with the same peak potential, but with a plateau that lasted 0·72 ms (thick trace), shown at faster time scale than in *A*. The calcium current was close to maximum with this waveform. *C*, peak amplitude of the calcium current during the repolarization phase *versus* plateau length. Amplitudes were normalized to the amplitude that was obtained with the standard action potential waveform, which was −2·9 nA (thick trace in *B*). Currents were filtered at 2 kHz before amplitudes were measured. ●, plateau phase to +60 mV. ○, plateau to +33 mV. Continuous line, fit of open symbols with an exponential function with a time constant of 0·35 ms.

steps. Because the duration of the action potential is so brief, compared with the speed of the voltage clamp in the axon, threshold (in this case a 40 mV depolarizationng step from the holding potential of −80 mV) is not reached for the calcium channels throughout most of the attached axon. The repolarization is much slower than during steps, and therefore the speed of the clamp becomes less critical and in our experiments was sufficiently fast. For the terminals in which a fast clamp could be established, the action potential-induced calcium currents did not depend on the length of the axon. Further evidence that the current we measured is representative of the current that enters during a normal action potential is that the calcium influx measured by a fluorescence method (Helmchen *et al.* 1997) is similar to the present results, both at room temperature (0·92 ± 0·05 *vs.* 0·96 ± 0·06 pC) and at physiological temperatures (0·81 ± 0·02 *vs.* 0·82 ± 0·05 pC) (see also (Borst & Helmchen, 1998).

Heterogeneity of presynaptic calcium currents in the calyx of Held

It was recently reported that 96 % of the calcium current in the calyx of Held flows though P/Q-type calcium channels (Takahashi, Forsythe, Tsujimoto, Barnes-Davies & Onodera, 1996). We find that the properties of the calcium currents were heterogeneous both with respect to steady-state inactivation (J. G. G. Borst & B. Sakmann, unpublished results), pharmacology (Wu *et al.* 1997) and activation (Fig. 3). At −30 mV, activation was fast, whereas at −20 mV it consisted of a fast and a slow component. The fast-activating component may represent the contribution from a different subtype of calcium channels. Nevertheless, in the HH simulations, we assumed that the calcium current originated from a single, homogeneous population of channels, meaning that our estimate for the open probability of the calcium channels during an action potential represents a mean value. The fast-activating current is likely to have a higher open probability during action potentials than the rest of the current, given its fast activation and its threshold for activation, which was slightly more negative than of the bulk calcium current.

Comparison with other calcium currents

The geometry of most nerve terminals makes them far from ideal for voltage clamp experiments. Therefore, limited voltage control has to be considered as an explanation for

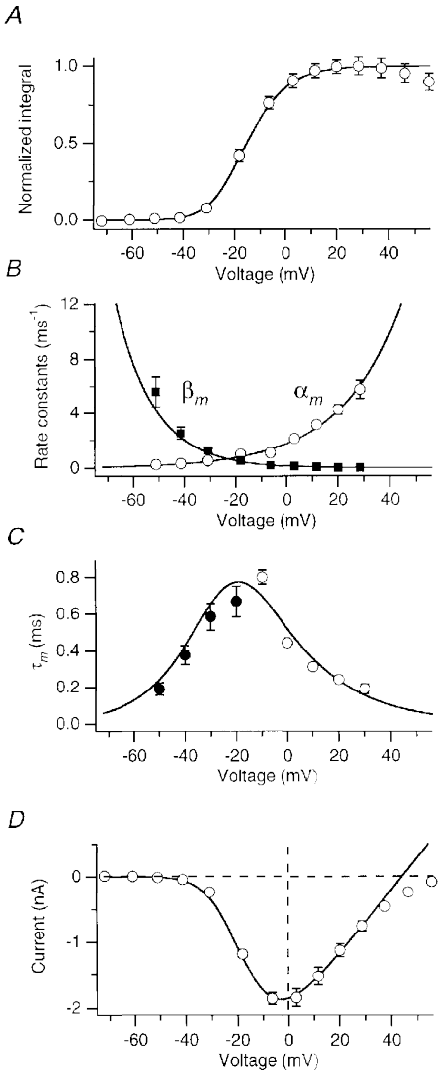

Figure 8. Hodgkin-Huxley model of calcium currents

A, averaged normalized tail current integrals after a 10 ms step ($n = 7$) were used as a measure for the average steady-state activation parameter $\bar{m}^2_\infty$. Integration time was 0·5 ms. Continuous line is a fit with a squared Boltzmann function (eqn (3)), with half-activation voltage, V_h, of −23·2 mV and steepness factor, κ, of 9·1 mV. *B*, rate constants for opening (α_m) and closing (β_m) of gate m. Continuous lines are the fits with a single exponential function (eqns (6) and (7)), with $\alpha_0 = 1{\cdot}78$ ms^{-1}, $V_\alpha = 23{\cdot}3$ mV and $\beta_0 = 0{\cdot}140$ ms^{-1}, $V_\beta = 15{\cdot}0$ mV, respectively. *C*, time constants (τ_m) measured from activation (○, eqn (2), $n = 7$) or deactivation (●, eqn (1), $n = 4$) of the calcium currents. The continuous line gives the time constants calculated from the rate constants of the HH model (shown in *B*), as $\tau_m = 1/(\alpha_m + \beta_m)$. *D*, average of the 7 *I–V* relations used for getting the steady-state activation and τ_m during the onset of the calcium currents. The continuous line is the fit with eqn (10) with maximal conductance $g_{max} = 48{\cdot}9$ nS and reversal potential $V_r = 43{\cdot}9$ mV.

the slow kinetics that were measured for some presynaptic calcium currents (Stanley & Goping, 1991; Wright, Brodwick & Bittner, 1996). Indeed, faster gating was reported more recently in the case of the ciliary ganglion (Yawo & Momiyama, 1993; Stanley & Mirotznik, 1997). Ribbon-type synapses such as the cochlear hair cells (Hudspeth & Lewis, 1988; Zidanic & Fuchs, 1995) or the bipolar cells of the retina (Mennerick & Matthews, 1996) are more readily voltage clamped and kinetics also were fast in these preparations. A comparison of the model described here with the model that Zidanic & Fuchs (1995) constructed for the chick cochlear hair cells and Llinás and co-workers (Llinás, Steinberg & Walton, 1981; Llinás *et al.* 1982) or Augustine (1990) for the presynaptic calcium current in the squid giant synapse shows that in both preparations gating is somewhat faster at positive potentials, but clearly slower at negative potentials than in the calyx of Held.

Gating kinetics of calcium channels in the calyx of Held were also clearly faster than of somatic calcium currents in mature guinea-pig hippocampus neurones (Kay & Wong, 1987), or adult bull-frog sympathetic neurones (Sala, 1991). In general, calcium channels in presynaptic terminals may show faster gating than those in the soma.

Presynaptic calcium current during an action potential

Because of the fast gating of the calcium channels, a presynaptic action potential is able to elicit a brief and large calcium influx. The shape of the calcium current is ideal for generating a large, localized increase in the calcium concentration at the membrane, as thought to be needed to trigger fast neurotransmitter release (Zucker, 1996). Because the presynaptic calcium current activates so fast, there is sufficient time during the upstroke of the action potential for most of them to open. The maximal increase in the amplitude of the currents when the peak of the action potential was prolonged was only 45%, without a change in the time course of the calcium current during the repolarization phase of the action potential, meaning that the open probability of the calcium currents is around 70% of maximal. The maximal open probability of the calcium channels in the calyx of Held is not known and variance analysis of ensemble currents or single channel recordings would be needed to obtain this value. Our estimate that the open probability during action potentials reaches 70% of maximal is subject to errors, since during longer steps calcium channels from the axon may have been recruited and both facilitation and inactivation of the calcium channels may have contributed. Nevertheless, this estimate was corroborated by results from the simulations. In the

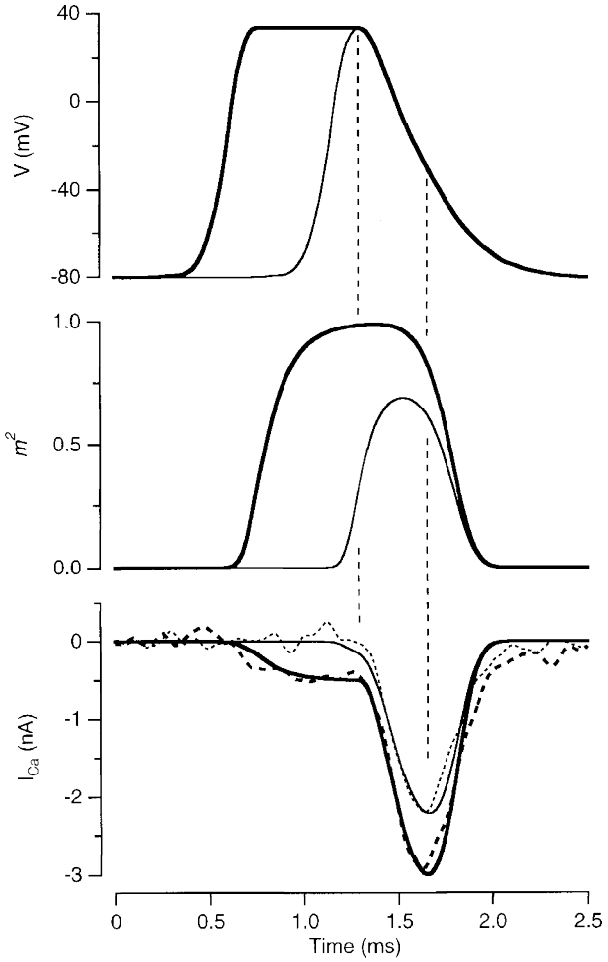

Figure 9. Simulation of calcium current during an action potential

Calcium currents were simulated with the HH model (eqn (8)). The standard action potential template (thin lines) was compared with the waveform that elicited the response shown in Fig. 7*B* (thick lines). Top, action potential waveforms. The vertical dotted lines give the peak of the action potential and the peak of the simulated calcium current. Middle, open probability (m^2) of the calcium channels during the normal action potential (thin line) and the action potential with the plateau phase (thick line). Bottom, currents. Thin line is the simulated current during the standard action potential. For comparison the measured calcium currents that were also shown in Fig. 7*B* (bottom) have been added (dotted lines). The experimental currents were both multiplied by 0·7 to normalize them to the simulated currents.

simulations, peak open probability was also around 70% of maximal, reached at a membrane potential of around −10 mV. The peak calcium current was reached shortly thereafter, at a membrane potential of −30 mV. At that point, open probability was still around 60% of maximal in the simulated currents. Obviously, the time course of the current during the repolarization phase results from the tradeoff between the increase of the driving force and the closure of the calcium channels due to the voltage-dependent deactivation kinetics.

Based on an HH model for the presynaptic calcium channels in the squid giant synapse, it was estimated that the peak open probability is only around 10% of maximal during 70 mV action potentials (Pumplin *et al.* 1981). The difference with the estimate of 70% for the calyx of Held is to a large extent due to the size of the action potentials. If an action potential of 80 mV (instead of 113 mV) is used in the simulations described in Fig. 9, the peak open probability also drops below 15%. Conversely, if calcium currents during the standard action potential waveform used here are simulated using the voltage-dependent rate constants from Llinás *et al.* (1982) or from Augustine (1990), peak open probability of the presynaptic invertebrate calcium channels would be 22% or 8% of maximal, respectively. This indicates that the differences in action potential waveform are not sufficient to explain the difference in the open probability. A direct comparison of the gating kinetics of the presynaptic calcium channels in the squid giant synapse and in the calyx of Held is difficult since the kinetics of the squid calcium channels were measured at a temperature which was 5–10 °C lower than for the calyx channels.

Time course of presynaptic calcium current at physiological temperature

At 36 °C, peak calcium currents were almost twice as large as at 24 °C. The peak amplitude was reached at a similar voltage as at room temperature. Since the half-width of the action potential was around half the value, the total calcium influx was slightly smaller at 36 °C than at 24 °C. The peak amplitude of the *I–V* relation increased by more than 50%. The slow deactivation at −20 mV and the results of the HH modelling suggest that at 24 °C few channels close before peak open probability is reached. Thus faster repolarization is insufficient to explain the difference. The Q_{10} (between 9 and 29 °C) of calcium channel conductance is only 1·2 (Lux & Brown, 1984), again insufficient to account for the increase at 36 °C. As calcium current activation seems to depend more strongly on temperature than deactivation (e.g. Lux & Brown, 1984; Nobile, Carbone, Lux & Zucker, 1990), it seems likely that the open probability of calcium channels during action potentials is even higher at physiological temperatures.

Sabatini & Regehr (1996) recently suggested that in cerebellar synapses at physiological temperature both calcium current and transmitter release begin early during the upstroke of action potentials. A puzzling result was that in their recordings the peak of the optically detected calcium current almost coincided with the peak of the action potential, meaning that the largest calcium current was seen when the driving force was very small. Nevertheless, some influx of calcium during the upstroke of the action potential was also observed at room temperature in varicosities from cultured motoneurones (Yazejian, DiGregorio, Vergara, Poage, Meriney & Grinnell, 1997) or in snail neurons that lack sodium currents (Gola, Hussy, Crest & Ducreux, 1986). Although we cannot exclude the possibility that a small calcium influx occurring before the peak of the action potential may have been obscured by the outward 'asymmetry' currents, a substantial influx would have been detected in our experiments. The calcium current still flowed during the repolarization phase at 36 °C. Sabatini & Regehr (1996, 1997) recorded the calcium influx from many terminals at the same time and it is not clear how they corrected for the jitter in the timing of the presynaptic action potentials in the different terminals. Indeed, the apparent time course of the calcium influx they measured at physiological temperatures was slower than what we observed at room temperature.

In the calyx of Held, both at room temperature and at physiological temperature, the calcium current had ended before the repolarization was complete. At both temperatures transmitter release begins late during repolarization of the presynaptic action potential (see Fig. 3 of Borst *et al.* 1995). This implies that calcium influx has largely ended before release begins, both at room temperature (Borst & Sakmann, 1996) and at physiological temperatures. The calcium concentration near the vesicles will rapidly decrease after channel closure. This indicates that most of the time delay between calcium influx and vesicle release is attributable to steps that follow the binding of calcium to the calcium sensor that is responsible for release (see also Zucker, 1996).

Conclusions

Because of the steep dependence of the amount of transmitter release in the MNTB on the size of the calcium influx (Borst & Sakmann, 1996; Wu *et al.* 1997), presynaptic calcium channels are a natural target for modulation by neurotransmitters (Takahashi *et al.* 1996). Although inhibition of calcium currents seems to be a more common mechanism than stimulation (Wu & Saggau, 1997), the open probability of calcium channels during a presynaptic action potential is not yet maximal, leaving open the possibility of both up and down modulation. Nevertheless, we find that the peak open probability is already close to maximal during normal action potentials. If calcium channels are clustered at the active zones, as in for example frog hair cells (Roberts, Jacobs & Hudspeth, 1990), the large influx of calcium during an action potential makes it likely that high concentrations of calcium are also reached in between the channels (Roberts, 1994). The large number of calcium channels that open with a probability that is close

to maximal may be important to minimize spatial variation in the peak calcium concentration near the membrane during consecutive action potentials, thereby reducing the contribution of the calcium channels to the variability in the size of the postsynaptic currents. In that case, vesicle release will be less dependent on their precise site of docking, since the vesicle does not have to be located right next to an open calcium channel.

Because the calcium influx through different channels is more likely to summate if adjacent calcium channels are open, our results are in agreement with a model of secretion in which most vesicles in the calyx of Held are released by the co-operative action of multiple calcium channels (Borst & Sakmann, 1996; Zucker, 1996).

Augustine, G. J. (1990). Regulation of transmitter release at the squid giant synapse by presynaptic delayed rectifier potassium current. *Journal of Physiology* **431**, 343–364.

Augustine, G. J., Charlton, M. P. & Smith, S. J. (1985). Calcium entry into voltage-clamped presynaptic terminals of squid. *Journal of Physiology* **367**, 143–162.

Bertram, R., Sherman, A. & Stanley, E. F. (1996). Single-domain/bound calcium hypothesis of transmitter release and facilitation. *Journal of Neurophysiology* **75**, 1919–1931.

Borst, J. G. G. & Helmchen, F. (1998). Calcium influx during an action potential. In *Methods in Enzymology*, ed. Conn, P. M. Academic Press (in the Press).

Borst, J. G. G., Helmchen, F. & Sakmann, B. (1995). Pre- and postsynaptic whole-cell recordings in the medial nucleus of the trapezoid body of the rat. *Journal of Physiology* **489**, 825–840.

Borst, J. G. G. & Sakmann, B. (1996). Calcium influx and transmitter release in a fast CNS synapse. *Nature* **383**, 431–434.

Brown, A. M., Tsuda, Y. & Wilson, D. L. (1983). A description of activation and conduction in calcium channels based on tail and turn-on current measurements in the snail. *Journal of Physiology* **344**, 549–583.

Byerly, L., Chase, P. B. & Stimers, J. R. (1984). Calcium current activation kinetics in neurones of the snail *Lymnaea stagnalis*. *Journal of Physiology* **348**, 187–207.

Delcour, A. H., Lipscombe, D. & Tsien, R. W. (1993). Multiple modes of N-type calcium channel activity distinguished by differences in gating kinetics. *Journal of Neuroscience* **13**, 181–194.

Dodge, F. A. Jr & Rahamimoff, R. (1967). Co-operative action of calcium ions in transmitter release at the neuromuscular junction. *Journal of Physiology* **193**, 419–432.

Forsythe, I. D. & Barnes-Davies, M. (1993). The binaural auditory pathway: excitatory amino acid receptors mediate dual timecourse excitatory postsynaptic currents in the rat medial nucleus of the trapezoid body. *Proceedings of the Royal Society* B **251**, 151–157.

Fröhr, F. (1985). *Electronic Control Engineering Made Easy, An Introduction for Beginners*. Siemens AG, Berlin and Munich, Germany.

Gola, M., Hussy, N., Crest, M. & Ducreux, C. (1986). Time course of Ca and Ca-dependent K currents during molluscan nerve cell action potentials. *Neuroscience Letters* **70**, 354–359.

Helfert, R. H. & Aschoff, A. (1997). Superior olivary complex and nuclei of the lateral lemniscus. In *The Central Auditory System*, ed. Ehret, G. & Romand, R., pp. 193–258. Oxford University Press, New York.

Helmchen, F., Borst, J. G. G. & Sakmann, B. (1997). Calcium dynamics associated with a single action potential in a CNS presynaptic terminal. *Biophysical Journal* **72**, 1458–1471.

Herrington, J. & Bookman, R. J. (1994). *Pulse Control V4.0: IGOR XOPs for Patch Clamp Data Acquisition and Capacitance Measurements*. University of Miami, Miami, FL, USA.

Hodgkin, A. L. & Huxley, A. F. (1952). A quantitative description of membrane current and its application to conductance and excitation in nerve. *Journal of Physiology* **117**, 500–544.

Hudspeth, A. J. & Lewis, R. S. (1988). Kinetic analysis of voltage- and ion-dependent conductances in saccular hair cells of the bull-frog, *Rana catesbeiana*. *Journal of Physiology* **400**, 237–274.

Katz, B. (1969). *The Release of Neural Transmitter Substances*. Thomas, Springfield, IL, USA.

Kay, A. R. & Wong, R. K. (1987). Calcium current activation kinetics in isolated pyramidal neurones of the CA1 region of the mature guinea-pig hippocampus. *Journal of Physiology* **392**, 603–616.

Kuwabara, N., DiCaprio, R. A. & Zook, J. M. (1991). Afferents to the medial nucleus of the trapezoid body and their collateral projections. *Journal of Comparative Neurology* **314**, 684–706.

Llinás, R., Steinberg, I. Z. & Walton, K. (1981). Presynaptic calcium currents in squid giant synapse. *Biophysical Journal* **33**, 289–321.

Llinás, R., Sugimori, M. & Simon, S. M. (1982). Transmission by presynaptic spike-like depolarization in the squid giant synapse. *Proceedings of the National Academy of Sciences of the USA* **79**, 2415–2419.

Lux, H. D. & Brown, A. M. (1984). Patch and whole cell calcium currents recorded simultaneously in snail neurons. *Journal of General Physiology* **83**, 727–750.

Mennerick, S. & Matthews, G. (1996). Ultrafast exocytosis elicited by calcium current in synaptic terminals of retinal bipolar neurons. *Neuron* **17**, 1241–1249.

Morest, D. K. (1968). The growth of synaptic endings in the mammalian brain: a study of the calyces of the trapezoid body. *Zeitschrift für Anatomie und Entwicklungsgeschichte* **127**, 201–220.

Neher, E. (1970). *Dynamische Eigenschaften von Nervensomamembranen*, p. 92. PhD Thesis, Technische Hochschule, Munich, Germany.

Nobile, M., Carbone, E., Lux, H. D. & Zucker, H. (1990). Temperature sensitivity of Ca currents in chick sensory neurones. *Pflügers Archiv* **415**, 658–663.

Pumplin, D. W., Reese, T. S. & Llinás, R. (1981). Are the presynaptic membrane particles the calcium channels? *Proceedings of the National Academy of Sciences of the USA* **78**, 7210–7213.

Roberts, W. M. (1994). Localization of calcium signals by a mobile calcium buffer in frog saccular hair cells. *Journal of Neuroscience* **14**, 3246–3262.

Roberts, W. M., Jacobs, R. A. & Hudspeth, A. J. (1990). Colocalization of ion channels involved in frequency selectivity and synaptic transmission at presynaptic active zones of hair cells. *Journal of Neuroscience* **10**, 3664–3684.

Sabatini, B. L. & Regehr, W. G. (1996). Timing of neurotransmission at fast synapses in the mammalian brain. *Nature* **384**, 170–172.

Sabatini, B. L. & Regehr, W. G. (1997). Control of neurotransmitter release by presynaptic waveform at the granule cell to Purkinje cell synapse. *Journal of Neuroscience* **17**, 3425–3435.

Sala, F. (1991). Activation kinetics of calcium currents in bull-frog sympathetic neurones. *Journal of Physiology* **437**, 221–238.

Stanley, E. F. & Goping, G. (1991). Characterization of a calcium current in a vertebrate cholinergic presynaptic nerve terminal. *Journal of Neuroscience* **11**, 985–993.

Stanley, E. F. & Mirotznik, R. R. (1997). Cleavage of syntaxin prevents G-protein regulation of presynaptic calcium channels. *Nature* **385**, 340–343.

Takahashi, T., Forsythe, I. D., Tsujimoto, T., Barnes-Davies, M. & Onodera, K. (1996). Presynaptic calcium current modulation by a metabotropic glutamate receptor. *Science* **274**, 594–597.

Toth, P. T. & Miller, R. J. (1995). Calcium and sodium currents evoked by action potential waveforms in rat sympathetic neurones. *Journal of Physiology* **485**, 43–57.

Wright, S. N., Brodwick, M. S. & Bittner, G. D. (1996). Presynaptic calcium currents at voltage-clamped excitor and inhibitor nerve terminals of crayfish. *Journal of Physiology* **496**, 347–361.

Wu, L.-G., Borst, J. G. G. & Sakmann, B. (1997). Multiple calcium channel types at a giant terminal in the mammalian CNS. *Society for Neuroscience Abstracts* **23**, 147.16.

Wu, L.-G. & Saggau, P. (1997). Presynaptic inhibition of elicited neurotransmitter release. *Trends in Neurosciences* **20**, 204–212.

Yawo, H. & Momiyama, A. (1993). Re-evaluation of calcium currents in pre- and postsynaptic neurones of the chick ciliary ganglion. *Journal of Physiology* **460**, 153–172.

Yazejian, B., DiGregorio, D. A., Vergara, J. L., Poage, R. E., Meriney, S. D. & Grinnell, A. D. (1997). Direct measurements of presynaptic calcium and calcium-activated potassium currents regulating neurotransmitter release at cultured *Xenopus* nerve-muscle synapses. *Journal of Neuroscience* **17**, 2990–3001.

Zidanic, M. & Fuchs, P. A. (1995). Kinetic analysis of barium currents in chick cochlear hair cells. *Biophysical Journal* **68**, 1323–1336.

Zucker, R. S. (1996). Exocytosis: a molecular and physiological perspective. *Neuron* **17**, 1049–1055.

Acknowledgements

We thank L.-G. Wu for discussions on slow tail currents and A. Roth, E. Neher and W. Almers for helpful comments on an earlier version of this manuscript. J.G.G.B. was supported by the EU (TMR fellowship).

Corresponding author

J. G. G. Borst, Max-Planck-Institut für medizinische Forschung, Abteilung Zellphysiologie, Jahnstrasse 29, D-69120 Heidelberg, Germany

Email: borst@sunny.mpimf-heidelberg.mpg.de